

A memristive model of spatio-temporal excitability

Thomas S.J. Burger, Amir Shahhosseini, Rodolphe Sepulchre

Abstract—This paper introduces a model of excitability that unifies the mechanism of an important neuronal property both in time and in space. As a starting point, we revisit both a key model of temporal excitability, proposed by Hodgkin and Huxley, and a key model of spatial excitability, proposed by Amari. We then propose a novel model that captures the temporal and spatial properties of both models. Our aim is to regard neuronal excitability as a property *across scales*, and to explore the benefits of modeling excitability with one and the same mechanism, whether at the cellular or the population level.

I. INTRODUCTION

Neuronal circuits function on spatial and temporal scales that span several orders of magnitude, from milliseconds to years, and from micrometers to dozens of centimeters. As just one example, neuron activity in the brain displays synchrony across multiple temporal and spatial scales, which has implications for a range of functions [1].

Modeling excitability has been a key focus of mathematical modeling in neuroscience since the seminal work of Hodgkin and Huxley in 1952 (see [2] and the recent textbooks [3], [4], [5]). The tradition has been, however, to adopt different modeling principles to capture excitability at different scales. The biophysical principles of Hodgkin and Huxley have been broadly adopted to model excitability at the level of a single neuron or for small circuits involving just a few neurons (for instance [6]). Instead, modeling excitability at the level of neuronal populations has been addressed with mean-field approaches (e.g. the model of Wilson and Cowan [7] and the model of Amari [8]). While cellular and population models of excitability share a number of qualitative properties, they are nevertheless of a different nature. Both cellular and mean-field models have been successful at describing neuronal behaviors at distinct scales, but the separate nature of the models has made it difficult to study excitability *across scales*, that is, to explore how cellular excitability mechanisms shape and modulate population excitability mechanisms. Attempts have been made to derive the macroscopic behavior from single-cell properties (see e.g. [9]), but at the price of starting from abstract neuron models that are difficult to relate to biophysical modeling principles.

Previous work by the authors, in particular [10] and the recent PhD dissertation [11] illustrate the shortcomings of modeling cellular and population activity with different modeling principles. In [10], the authors show how neuromod-

ulators can shape spatio-temporal activity (“brain states”) by modulating the intrinsic properties of the neurons rather than the synaptic neural connections. In [11], the author demonstrates how particular properties at the cellular scale determine the robustness of the mean-field PING rhythm at the population scale. In both examples, a population phenomenon is regulated at the cellular scale, and the only way to study the mechanism “across scales” is to simulate the entire population at the neuronal scale, which is cumbersome and not scalable.

Motivated by those shortcomings, we aim at developing new population models that will make it easier to study neuronal behaviors across scales. As a first step in that direction, we propose a spatio-temporal model that unifies the temporal model of Hodgkin and Huxley and the spatial model of Amari.

Our angle of attack is to retain the key biophysical modeling principles of Hodgkin and Huxley, namely the circuit representation of each neuron as the parallel connection of a capacitive element with a bank of voltage-gated current sources. In the original model of Hodgkin and Huxley, the current sources are *memristive*, that is, they obey an Ohmic law but with conductances that have memory, that is, depend on the history of the voltage. In the present paper, such conductances with memory are called *memductances*, following the terminology of [12]. The proposed standpoint is that this memristive modelling principle is valid both at the cellular and the population scale, and that only the model of the memductance differs. We then exploit the close analogy between ion channels (i.e. *internal* memductances) and synapses (i.e. *external* memductances) to model their temporal and spatial voltage dependence.

We stress the advantages of a simple circuit model that concentrates all the temporal and spatial modeling complexity in the spatio-temporal voltage dependence of the memductances. Simplified models preserve the same physical circuit structure but use simplified representations of the memductances. Temporal models spatially average the spatial dependence, while spatial models temporally average the voltage dependence. We argue that such models can be simulated, analyzed, and designed *at scale* by modulating the model resolution of the memductances only.

The paper is structured as follows. In Section II, we review the Hodgkin Huxley model of temporal excitability. Section III revisits Amari’s model of lateral inhibition, which we regard as spatial excitability. The unified memristive model is introduced in Section IV. We show that simple models of the memductances capture both temporal and spatial excitability, either separately or together.

KU Leuven, Department of Electrical Engineering (ESAT), STADIUS Center for Dynamical Systems, Signal Processing and Data Analytics, Kasteelpark Arenberg 10, 3001 Leuven, Belgium
thomas.burger@kuleuven.be

II. TEMPORAL EXCITABILITY

The biophysical foundation of neuroscience, and therefore of our understanding of excitable behaviors, is the work of Hodgkin and Huxley, culminating in [2].

The key modeling principle is that a neuron can be represented by an RC circuit in parallel with a bank of voltage-gated current sources. Temporal excitability only requires two such sources, as shown in Equation 1. The capacitor models the membrane of the neuron, because there is a voltage difference between the inside of the cell and the extracellular medium. This voltage changes as ions flow in and out through the cell membrane. The flow of each ion is controlled by a specific ion channel, modeled as an Ohmic current whose conductance is voltage-dependent due to the voltage-dependent opening and closing of channels at the microscopic level.

In Hodgkin and Huxley's model, only two ion channels are present: sodium (Na) and potassium (K). The remaining channels are gathered in a passive 'leak' current i_l . The applied current i_{app} models "external" currents, for instance resulting from synaptic connections to other neurons. The equations of the Hodgkin-Huxley model are:

$$\begin{aligned} C\dot{v} &= -(i_l + i_{Na} + i_K) + i_{app} \\ i_l &= g_l(v - E_l) \\ i_{Na} &= g_{Na}m^3h(v - E_{Na}) \\ i_K &= g_Kn^4(v - E_K). \end{aligned} \quad (1)$$

Here, v is the voltage over the cell membrane, C is the capacitance of the membrane, g_k denotes the memductance of the current flowing through the ion channel of type k , and E_k is the equilibrium (or Nernst) potential of this channel.

The temporal voltage-dependence of the ionic memductances of sodium and potassium is modeled through additional state variables that model the activation and inactivation of the current. In the Hodgkin-Huxley model, the ionic memductance of ion k is modeled by

$$g_k(t, v) = \bar{g}_k m_k^a h_k^b, \quad (2)$$

for some $a, b \in \mathbb{N}$ and a maximal conductance $\bar{g}_k > 0$. Here, m and h both have first-order dynamics

$$\dot{x} = (x_\infty(v) - x) / \tau_x(v), \quad (3)$$

where $x_\infty(v) \in [0, 1]$ is a sigmoidal function, and $\tau_x(v)$ is either bell-shaped or U-shaped, depending on the ion in question. m is called an activation variable because $m_\infty(v)$ increases monotonically with v (that is, it models the channel opening as v increases), and h is called an inactivation variable as $h_\infty(v)$ decreases monotonically (it models the channel closing as v increases). For the sodium channel in the Hodgkin-Huxley model $a = 3$ and $b = 1$ and for the potassium channel $a = 4$ and $b = 0$.

The feedback structure of the model is sketched in Figure 2. First, the voltage goes through a nonlinearity x_∞ for $x = m, n, h$. The resulting quantity goes through a nonlinear temporal convolution with an exponential kernel $e^{-t/\tau_x(v)}$ to give the gating variables. These two steps capture Equation

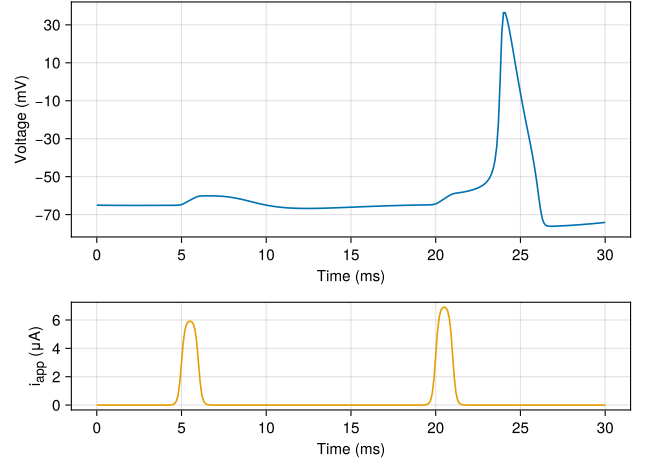


Fig. 1. Temporal excitability in the Hodgkin-Huxley model. A small difference in i_{app} (bottom) can cause a large difference in the voltage response (top).

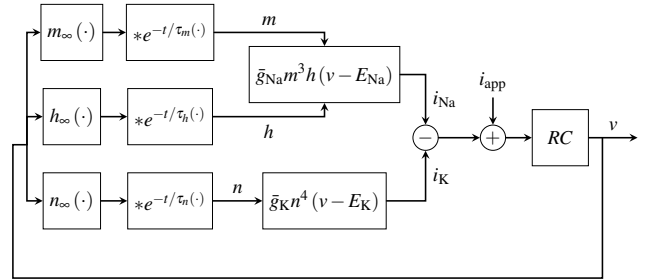


Fig. 2. Block diagram of the mixed temporal monotone structure of the Hodgkin-Huxley model.

3. Then, these gating variables go through polynomials that give the ionic currents, which go through the RC circuit to determine v .

The Na and K ion channels together are sufficient to generate temporally excitable behaviors: a stereotyped, brief large-amplitude response when the input stimulus exceeds some threshold in frequency or amplitude, as illustrated in Figure 1. The fast activation of the sodium current provides positive feedback on v , causing it to act as a switch. This fast switching behavior is captured in the model by m , specifically through $m_\infty(v)$ increasing monotonically and $\tau_m(v)$ being small compared to τ_n and τ_h , together with E_{Na} being much bigger than the resting potential of the neuron v_{rest} so that $i_{Na} < 0$ for normal voltage values of the neuron. But this switch is then turned off through the much slower inactivation of sodium (modeled by h) and activation of potassium (modeled by n), which provide negative feedback on v . This motif of fast positive feedback paired with slower negative feedback for global stability creates a region where the model is ultra-sensitive: this is the threshold, which lies at the heart of excitable behaviors in time.

III. SPATIAL EXCITABILITY

Information in the brain is routed and shared through many synaptic stages and brain areas. In the brain, the spatial extent

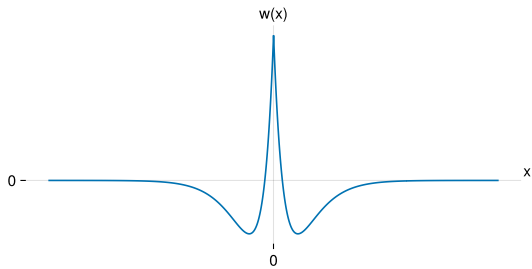


Fig. 3. Sketch of $w(x)$ as used in Amari's model.

of activity is mediated through a zoo of neurons, which can be broadly characterized into two classes: excitatory (E) and inhibitory (I). Excitatory neurons promote further neuronal activity, whilst inhibitory neurons usually diminish it. Excitation and inhibition are spatially structured, with E and I operating in a balanced regime. This can lead to interesting spatial patterns, such as oscillations, in the neuronal activity. Two foundational models of this are [7] and [8].

In Amari's model [8], spatial interactions are modeled as a simple spatial convolution operator. The spatio-temporal membrane potential is now $u(x,t)$. The output (which models the average firing rate) is given by $f(u(x,t))$ for some monotonically non-decreasing f . We use $f(x) = 1/(1 + \exp(-5(u - \theta)))$, where θ is the firing threshold. Then the neural field evolves according to

$$\tau \dot{u} = -u + \int_{\Omega} w(x-y) f(u(y,t)) dy + i_{\text{app}}, \quad (4)$$

where $w(x-y)$ represents the average connection strength from neurons at y to neurons at x , Ω is the region of the neural field, and τ is the membrane time constant.

The spatial interactions between neurons in the field are therefore determined by $w(x)$. It is sketched in Figure 3. Excitatory connections are those connections that lead to an increase in \dot{v} , whereas inhibitory connections decrease \dot{v} . The salient features of the interaction kernel are that the excitation ($w(x) > 0$) is short-range, whereas inhibition ($w(x) < 0$) is longer range.

When the kernel is defined as the difference of exponentials $w(x) = e^{-|x|/\sigma_E} - e^{-|x|/\sigma_I}$, the feedback structure of Amari's model can be represented as in Figure 5. The averaged potential u goes through f , the result is convolved in space with two kernels with different parameters σ , defining the length scale of the interactions. We require $\sigma_E < \sigma_I$ to preserve the difference in length scales between the E and I interactions. Then, $i_E - i_I + i_{\text{app}}$ goes through the RC block to produce u . The reader will note the analogy with the block diagram of Hodgkin-Huxley model (Figure 2): in both models, the voltage-dependent currents create a mixed-feedback model, that is, the feedback controller is the difference of two currents. The models only differ in how they model the voltage dependence of the currents: temporal nonlinear convolution with an exponential kernel in Hodgkin-Huxley model and spatial convolution with an exponential kernel in Amari's model.

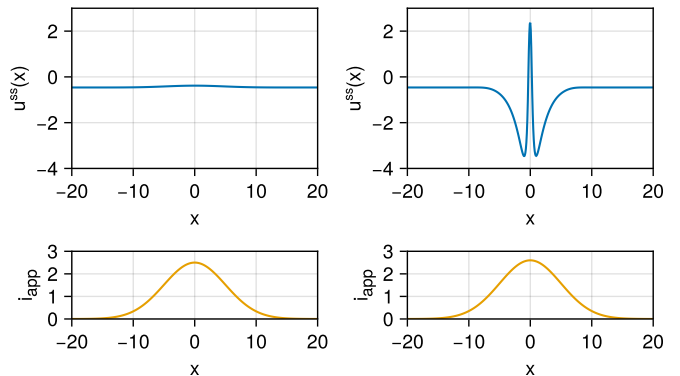


Fig. 4. Spatial excitability in Amari's model. Left: the subthreshold steady-state voltage response $u^{ss}(x)$ (top) to Gaussian input current (bottom). Right: The suprathreshold steady-state voltage response $u^{ss}(x)$ (top) to a Gaussian input current (bottom). The first applied pulse does not lead to spatial excitation, whereas the second applied pulse does,

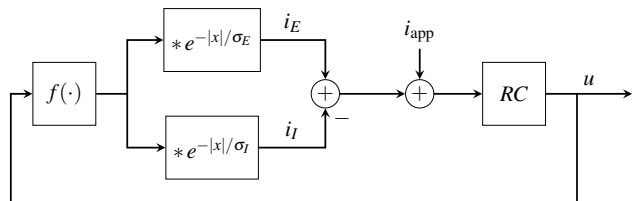


Fig. 5. Block diagram of the mixed spatial monotone structure of Amari's model. We require $\sigma_E < \sigma_I$ to ensure that the excitatory interactions given by i_E operate on shorter length scales than the inhibitory interactions given by i_I .

As in the Hodgkin-Huxley model, the mixed-feedback structure of Amari's model is key to its spatial excitability: when the neural mass exceeds a threshold, the feedback mechanism leads to a spatially localized 'event' or 'spike'. Namely, the non-equilibrium behavior consists of one or more regions with a certain width, determined by the spatial kernel w , that switch 'on', thereby inhibiting the rest of the field.

This is demonstrated in Figure 4, where we have plotted the steady-state after relaxation $u^{ss}(x)$ in response to two Gaussian input pulses $i_{\text{app}}(x,t)$, both wide in space and time. The first pulse does not cause v to exceed its threshold, and the response is small. The second pulse triggers an excitation in u which is much narrower in space than the pulse, and persistent in time. Many more complicated static and dynamical patterns can be supported, such as oscillations and traveling waves [8]. Spatial excitability is the system's ability to support these patterns reliably based on the statistics of the excitatory and inhibitory connections within the circuit.

IV. MEMRISTIVE MODELING

Based on the mixed-feedback analogy between the temporal excitability of the Hodgkin-Huxley model and the spatial excitability of Amari's model, we introduce a unified model that captures both temporal and spatial excitability. We retain the two important elements from the Hodgkin-Huxley model (Equation 1). First, each current is memristive [12]: the value of the current at time t and position x equals the membrane

voltage at time t and position x , multiplied by a memductance that depends on the entire neural field, or more precisely the entire past of the entire spatial neural field. Each memristive current is possibly in series with a constant voltage battery, resulting in a current source of the form $i = g(v - v_0)$ for some constant v_0 .

Secondly, we retain the mixed feedback motif shown in Figure 2 as the crucial mechanism for excitable behaviors.

Mimicking the architecture of the Hodgkin-Huxley model, we include one single inward current, labeled e , and one single outward current, labeled i . The excitatory e current models the fast Na current in Hodgkin-Huxley and l or the short ranged current in Amari, while the inhibitory i current models the slow K current and l or the long ranged current.

The voltage dynamics are that of a nonlinear RC circuit, with the addition of a spatial dependence:

$$\begin{aligned} C\dot{v} &= -i_{\text{tot}} \\ &= -g_l v - g_e(x, t)(v - E_e) - g_i(x, t)(v - E_i) \end{aligned} \quad (5)$$

The entire spatio-temporal complexity of the model goes into the modeling of the g_e and g_i memductances. Memductances must be nonlinear, because they modulate the current between zero (completely closed channels) and a maximum conductance \bar{g} (completely open channels). The temporal dependence of the memductance must be “fast” or “slow”, which we capture by a simple temporal convolution operation with decaying exponentials characterized by a specific time scale. Likewise, the spatial dependence of the memductance must be “short-range” or “long-range”, which we capture with a simple spatial convolution with decaying exponentials characterized by a specific spatial scale.

The core observation is that the memductance of each current can be modeled as a nonlinear convolution operator, typically in the form of a Convolution Neural Network (CNN) model. The complexity of a particular instantiation of the model is only determined by the complexity of this *feedforward* neural network operator. In the next sections we will illustrate that simple models of the memductance suffice to capture temporal and spatial excitability.

A. A model of temporal excitability

In Section II, we discussed how temporal excitability is the result of fast positive feedback on the membrane potential followed up with slower negative feedback. How difficult is it to model such memristive properties with a CNN model?

To obtain temporal excitability, we restrict g_e and g_i to the time domain and only give them activation variables m . The e current must provide fast positive feedback, so $E_e > 0$ and $\tau_{e,m} < \tau_{i,m}$. The i current must give slow negative feedback, so $E_i < 0$. The model is

$$\begin{aligned} \tau_{e,m}\dot{v}_e &= v - v_{e,m} \\ g_e &= \bar{g}_e \text{relu}(v_{e,m} - v_{e,m}^{\text{th}}) \\ \tau_{i,m}\dot{v}_i &= v - v_{i,m} \\ g_i &= \bar{g}_i \text{relu}(v_{i,m} - v_{i,m}^{\text{th}}). \end{aligned} \quad (6)$$

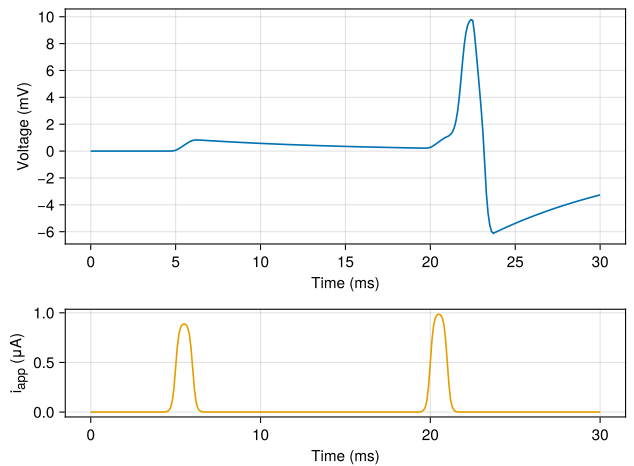


Fig. 6. Temporal excitability of the memristive neuron model. A small increase in i_{app} brings the voltage over its threshold, resulting in a large pulse-like voltage trajectory (top). This threshold behavior is qualitatively equivalent to the excitability of Hodgkin-Huxley model, cf. Figure 1.

together with Equation 5. Here, the $\tau_{x,m}$ are the time constants of the memductances and $v_{x,m}^{\text{th}}$ are their thresholds. Implementing this with the parameters given in Table III yields a firing threshold analogous to that of biophysical models, which is demonstrated in Figure 6.

Due to the model’s simplicity, we can determine the conditions for excitability. Consider the model starting from rest with $v = v_e = v_i = 0$ and i_{app} being applied at $t = 0$ with sufficient energy to push v above $v_{e,m}^{\text{th}}$. To get positive feedback, we require $di_{\text{tot}}/dv < 0$. As $\tau_{e,m} < \tau_{i,m}$, we have $v_{e,m} \approx v$, but $v_{i,m}$ remains close to rest: $v_{i,m} \approx 0$. Then $i_{\text{tot}} \approx g_l v + \bar{g}_e (v - v_{e,m}^{\text{th}})(v - E_e)$, so $di_{\text{tot}}/dv \approx g_l + \bar{g}_e (2v - E_e - v_{e,m}^{\text{th}})$, and the criterion for positive feedback becomes

$$v_{e,m}^{\text{th}} < v < \frac{1}{2} \left(-\frac{g_l}{\bar{g}_e} + E_e + v_{e,m}^{\text{th}} \right). \quad (7)$$

When $v > v_{i,m}^{\text{th}}$ and both the e and i currents have activated, we require negative feedback, so $di_{\text{tot}}/dv > 0$. The derivative becomes $di_{\text{tot}}/dv = g_l + 2(\bar{g}_e - \bar{g}_i)v - \bar{g}_e(v_{e,m}^{\text{th}} + E_e) - \bar{g}_i(v_{i,m}^{\text{th}} + E_i)$ and the criterion for positive differential conductance (negative feedback) with both channels active is

$$v > \max \left\{ \frac{\bar{g}_e(E_e + v_{e,m}^{\text{th}}) + \bar{g}_i(E_i + v_{i,m}^{\text{th}}) - g_l}{2(\bar{g}_e + \bar{g}_i)}, v_{e,m}^{\text{th}}, v_{i,m}^{\text{th}} \right\}. \quad (8)$$

The mechanism described above is robust to uncertainty in the parameter values; excitability only requires an E_e sufficiently large so that Equation 7 is satisfied, and then a $\bar{g}_i > \bar{g}_e$ and sufficiently negative E_i so that Equation 8 is satisfied for all $v > 0$. This will ensure that there is a region of negative differential conductance (that is, positive feedback) in the fast timescale and positive differential conductance (negative feedback) overall. Temporal excitability is the result of this mixed-feedback structure, as Figure 6 shows.

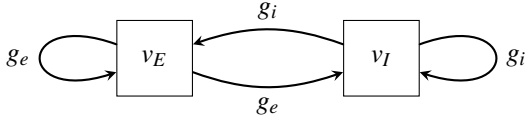


Fig. 7. Relationship between v_E , v_I and g_e , g_i to model spatial excitability.

B. A model of spatial excitability

Amari’s model exhibits the same mixed-feedback structure as the Hodgkin-Huxley model. However it is not memristive, that is, the feedback currents are not Ohmic.

To obtain a memristive model of spatial excitability, we retain the key properties of Amari’s model: we choose as our spatial filter

$$w(x) = e^{-|x|/\sigma}, \quad (9)$$

where the parameter σ again controls the spatial scale of the interactions. Because the kernel w now defines a memductance, and not a current (as with Amari), it must be nonnegative.

Therefore, to differentiate between excitation and inhibition, we separate the neural field into excitatory and inhibitory populations which we label E and I , with membrane voltages v_E and v_I . To examine how this can lead to spatial excitability, we model g_e and g_i as synaptic currents between the E and I populations, with their memductances following

$$\begin{aligned} \tau_{\text{syn}} v_{\text{syn},t} &= v - v_{\text{syn},t} \\ v_{\text{syn},st} &= (v_{\text{syn},t} * w)(x,t) \\ g_{\text{syn}}(x,t) &= \bar{g}_{\text{syn}} \text{relu}(v_{\text{syn},st} - v_{\text{syn}}^{\text{th}})(x,t), \end{aligned} \quad (10)$$

where the subscript t denotes the temporally filtered v_{syn} , and the subscript s denotes the spatially filtered field, $v_{\text{syn}}^{\text{th}}$ is the memductance’s threshold, and $*$ denotes the operation of the spatial convolution.

Each population is connected to itself and to the other, meaning that the g_e memductance for both \dot{v}_E and \dot{v}_I takes v_E as input, and analogously g_i takes v_I as input for both populations, as is depicted in Figure 7.

To obtain local excitation with long-range inhibition the σ parameters of the memductance kernels are adjusted for the excitatory and inhibitory synapses, so that $\sigma_E < \sigma_I$. Similarly, following physiological data, we choose $\tau_{E,\text{syn}} < \tau_{I,\text{syn}}$, so that synaptic excitation works faster than synaptic inhibition.

The steady-state voltage response of the E population in the spatial memristive model with the parameters given in Table IV to two different i_{app} currents is shown in Figure 8. The first pulse is subthreshold, which elicits a small and brief response. The second pulse, although only slightly higher in amplitude, is superthreshold. As in Figure 4 with Amari’s model, the upshot is a localized persistent bump in activity. This shows that a simple spatial CNN model of memductances is sufficient to model spatial excitability.

V. SPATIO-TEMPORAL EXCITABILITY

To obtain a model of spatio-temporal excitability, we simply combine the temporal mechanism from Section IV-A and

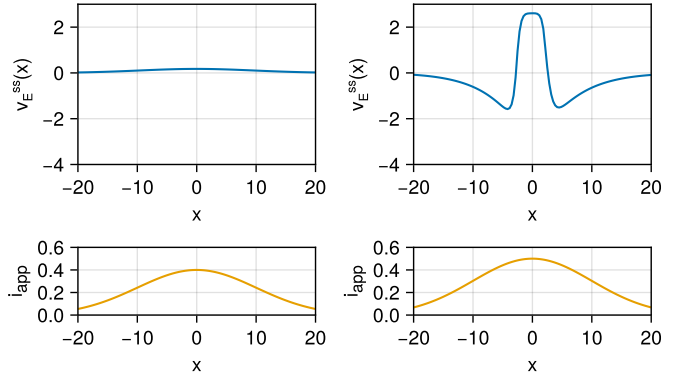


Fig. 8. Spatial excitability in the CNN model. Left: the subthreshold steady-state voltage response $v_E^{ss}(x)$ (top) to Gaussian input current (bottom). Right: The superthreshold steady-state voltage response $v_E^{ss}(x)$ (top) to a Gaussian input current (bottom). The first applied pulse does not lead to spatial excitation, whereas the second applied pulse does, cf. Figure 4.

the spatial mechanism from Section IV-B. The membrane potential of population k evolves according to

$$\begin{aligned} C\dot{v}_k &= -g_I v_k - (g_e(x,t) + g_{e,\text{syn}}(x,t))(v_k - E_e) \\ &\quad (g_i(x,t) + g_{i,\text{syn}}(x,t))(v_k - E_i) + i_{\text{app}}, \end{aligned} \quad (11)$$

where $k \in \{E, I\}$ indicates the E and I population and, as before, g_e and g_i are the temporal memductances with the parameters from Table III, and the dynamics of $g_{e,\text{syn}}$ and $g_{i,\text{syn}}$ are dependent on v_E and v_I respectively and give the network interactions.

The resulting model unifies the temporally excitable behavior of the Hodgkin-Huxley model and the spatially excitable behavior of Amari’s model (Figure 9). The purely temporal currents have the biophysical interpretation of *internal* memductances, or ion channels, that is, the memductance at position x depends on the voltage at x only. The spatial currents have the biophysical interpretation of synaptic currents: they obey the same Ohmic law as internal memductances, with the only difference that their memductance depends on “pre-synaptic” voltages, that is, on the voltage of other neurons in the population.

VI. CONCLUSIONS AND FUTURE WORK

A. Conclusions

Temporal excitability is the result of fast positive feedback tempered by slower negative feedback on the membrane potential. Spatial excitability is the result of short-ranged excitatory connections coupled with longer ranged inhibitory connections to limit the excitation and overall activity. Our paper proposes a methodology that unifies the modeling principles of those two behaviors.

The architecture of the proposed model retains key properties of the biophysical model of Hodgkin and Huxley: a neuron is modeled as an RC circuit controlled by a bank of parallel voltage-gated current sources. The only part of the model that differentiates its temporal and spatial scales is in the memductances, that is, the mapping from the entire neural field $v(x,t)$ to a specific memductance.

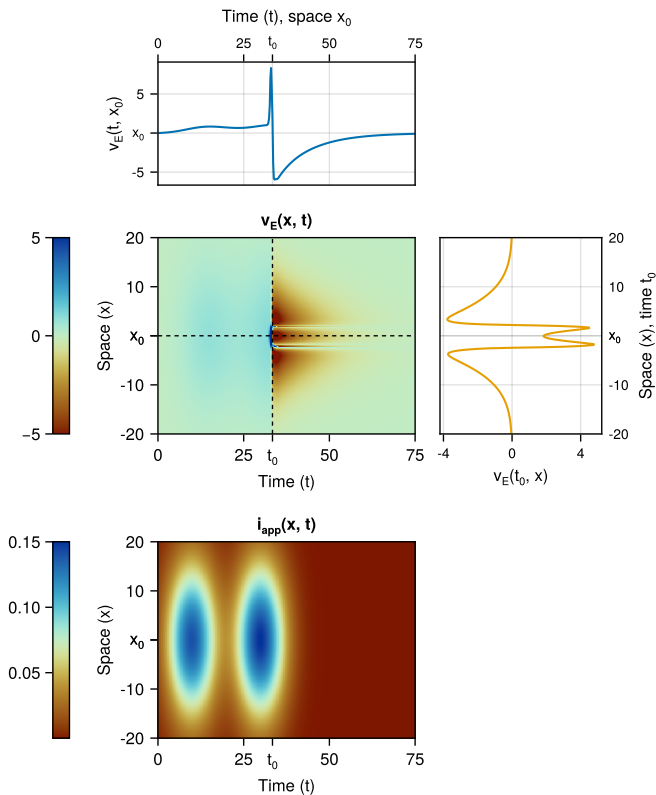


Fig. 9. Spatio-temporal excitability in the canonical model. The response of the excitatory voltage $v_E(x, t)$ (central top figure) in response to an applied current $i_{app}(x, t)$ (bottom figure). The temporal profile of v_E at $x_0 = 0$ is plotted in the upper inset, whilst the spatial profile of v_E along $t_0 = 33$ is plotted in the upper-right inset. The temporal profile shows temporally excitable behavior (cf. Figure 1) and the spatial profile shows spatial excitability (cf. Figure 4).

The proposed model highlights that the mechanism of excitability is only the result of a mixed-feedback architecture that is analogous in time and in space. The excitability property is robust to the details of the memductance model, meaning that excitability can be simulated, analyzed, and designed at different scales.

A key benefit of the proposed model is that it retains the full biophysical interpretability of traditional biophysical models. Purely temporal memductances have the interpretation of ion channels, that is, the voltage dependence is only temporal but not spatial, whereas spatial currents retain the interpretation of synaptic currents, whose memductance is gated by other neurons in the population.

B. Future Work

While preliminary, the results of this paper have significant potential to simulate, analyze, and design neuronal behaviors across scales.

The mixed-feedback and biophysical architecture of the model should facilitate the generalization of the excitability property in this paper to more complex behaviors. For instance, we expect a smooth generalization from spiking to bursting behaviors using the multi-scale mixed feedback architecture highlighted for instance in [13] and references

therein.

We also envision a significant potential for a framework that is algorithmically scalable. Large-scale simulations of memristive models will rely on the operator-theoretic framework developed in [14] and [15]. The methodology in those papers is to solve the neural field as the fixed point of an operator in the space of current-voltage trajectories rather than by integration in time and space. The framework makes uses of efficient splitting methods that can leverage the highly parallel structure of neuronal circuits and their decomposition in simple elements.

VII. APPENDIX

For the Hodgkin-Huxley model in Figure 1, the parameters in Table I were used.

TABLE I
HODGKIN-HUXLEY MODEL CONDUCTANCE AND REVERSAL POTENTIAL PARAMETERS.

\bar{g}_{Na}	E_{Na}	\bar{g}_K	E_K	\bar{g}_L	E_L
120	50	36	-77	0.3	-54.4

For Amari's model and w for Figure 4, the parameters in Table II were used.

TABLE II
AMARI'S MODEL PARAMETERS.

τ	σ_E	σ_I	θ
3	0.3	2	0.4

The parameters of the memristive neuron model with temporal excitability used in Figures 6 and 9 are given in Table III. Wherever applicable, $C = 1$.

TABLE III
PARAMETERS FOR TEMPORAL EXCITABILITY IN THE CNN MODEL.

g_I	$\tau_{e,m}$	\bar{g}_e	E_e	$v_{e,m}^{th}$	\bar{g}_i	$\tau_{i,m}$	E_i	$v_{i,m}^{th}$
0.1	0.1	1	10	1	10	10	-10	1

The parameters of the CNN model with spatial excitability, used in Figures 8 and 9 are given in Table IV.

TABLE IV
PARAMETERS FOR SPATIAL EXCITABILITY IN THE CNN.

g_I	σ^E	τ_{syn}^E	v_E^{th}	\bar{g}_{syn}^E	E_{syn}^E	σ^I	τ_{syn}^I	v_I^{th}	\bar{g}_{syn}^I	E_{syn}^I
0.1	0.5	0.1	2	10	10	5	1	2	3	-10

The applied current followed $i_{app}(x, t) = i_{pulse}^{(1)} + i_{pulse}^{(2)}$ where $i_{pulse}(x, t) = A \exp\left(-\frac{x^2}{2\sigma_x^2}\right) \exp\left(-\frac{(t-t_0)^2}{2\sigma_t^2}\right)$. For Figures 4, 8, and 9, the i_{app} parameters from Table V were used.

For Figure 4 values u^{ss} were read off at $t = 205$ and $t = 305$.

For Figure 8 values for v_E^{ss} were read off at $t = 100$ and $t = 200$.

TABLE V

STIMULATION PARAMETERS OF i_{APP} USED IN FIGURES 4, 8, AND 9.

Figure	$A^{(1)}$	$A^{(2)}$	σ_x	σ_r	$t_0^{(1)}$	$t_0^{(2)}$
4	2.5	2.6	5.0	5.0	10	210
8	0.4	0.5	10	5	5	105
9	0.14	0.15	10	5	10	30

VIII. ACKNOWLEDGMENTS

This work was supported by funding from the European Research Council under the European Union’s Horizon 2020 research and innovation program / ERC Advanced Grant: SpikyControl (no. 7101054323), and by reviewer’s comments, both of which we are grateful for.

REFERENCES

- [1] M. J. Kahana, “The Cognitive Correlates of Human Brain Oscillations,” *Journal of Neuroscience*, vol. 26, pp. 1669–1672, Feb. 2006.
- [2] A. L. Hodgkin and A. F. Huxley, “A quantitative description of membrane current and its application to conduction and excitation in nerve,” *The Journal of Physiology*, vol. 117, pp. 500–544, Aug. 1952.
- [3] J. Keener and J. Sneyd, “Mathematical physiology 1: Cellular physiology,” 2009.
- [4] E. M. Izhikevich, *Dynamical systems in neuroscience*. MIT press, 2007.
- [5] B. Ermentrout and D. H. Terman, *Foundations of mathematical neuroscience*. Citeseer, 2010.
- [6] F. Buchholtz, J. Golowasch, I. R. Epstein, and E. Marder, “Mathematical model of an identified stomatogastric ganglion neuron,” *Journal of neurophysiology*, vol. 67, no. 2, pp. 332–340, 1992.
- [7] H. R. Wilson and J. D. Cowan, “Excitatory and Inhibitory Interactions in Localized Populations of Model Neurons,” *Biophysical Journal*, vol. 12, pp. 1–24, Jan. 1972.
- [8] S.-i. Amari, “Dynamics of pattern formation in lateral-inhibition type neural fields,” *Biological Cybernetics*, vol. 27, pp. 77–87, June 1977.
- [9] S. Coombes and Á. Byrne, “Next Generation Neural Mass Models,” in *Nonlinear Dynamics in Computational Neuroscience* (F. Corinto and A. Torcini, eds.), pp. 1–16, Cham: Springer International Publishing, 2019.
- [10] G. Drion, J. Dethier, A. Franci, and R. Sepulchre, “Switchable slow cellular conductances determine robustness and tunability of network states,” *PLoS computational biology*, vol. 14, no. 4, p. e1006125, 2018.
- [11] T. Burger, *Oscillatory Spiking Circuits: A biologically plausible architecture for fast and reliable spiking computations*. Ph.d. thesis, University of Cambridge, Cambridge, United Kingdom, 2023.
- [12] L. Chua and S. M. Kang, “Memristive devices and systems,” *Proceedings of the IEEE*, vol. 64, pp. 209–223, Feb. 1976.
- [13] L. Ribar and R. Sepulchre, “Neuromorphic control: Designing multiscale mixed-feedback systems,” *IEEE Control Systems Magazine*, vol. 41, no. 6, pp. 34–63, 2021.
- [14] T. Chaffey and R. Sepulchre, “Monotone one-port circuits,” *IEEE Transactions on Automatic Control*, vol. 69, no. 2, pp. 783–796, 2023.
- [15] A. Shahhosseini, T. Chaffey, and R. Sepulchre, “An operator-theoretic framework to simulate neuromorphic circuits,” in *2024 IEEE 63rd Conference on Decision and Control (CDC)*, pp. 6703–6708, IEEE, 2024.